



HAL
open science

Effect of halogenation on the optical and electronic properties of tetrathienoanthracene and tetrathionoacridine derivatives: A DFT study

Koussai Lazaar, Moncef Said, Michael Badawi, Sébastien Lebègue, Saber Gueddida

► To cite this version:

Koussai Lazaar, Moncef Said, Michael Badawi, Sébastien Lebègue, Saber Gueddida. Effect of halogenation on the optical and electronic properties of tetrathienoanthracene and tetrathionoacridine derivatives: A DFT study. *Computational Condensed Matter*, 2021, 26, pp.e00528 -. 10.1016/j.cocom.2020.e00528 . hal-03492759

HAL Id: hal-03492759

<https://hal.science/hal-03492759>

Submitted on 2 Jan 2023

HAL is a multi-disciplinary open access archive for the deposit and dissemination of scientific research documents, whether they are published or not. The documents may come from teaching and research institutions in France or abroad, or from public or private research centers.

L'archive ouverte pluridisciplinaire **HAL**, est destinée au dépôt et à la diffusion de documents scientifiques de niveau recherche, publiés ou non, émanant des établissements d'enseignement et de recherche français ou étrangers, des laboratoires publics ou privés.



Distributed under a Creative Commons Attribution - NonCommercial 4.0 International License

Effect of halogenation on the optical and electronic properties of tetrathienoanthracene and tetrathionoacridine derivatives: a DFT study

Koussai Lazaar^a, Moncef Said^a, Michael Badawi^b, Sébastien Lebègue^b, Saber Gueddida^{b,*}

^a *University of Monastir, LMCN (LR11ES40), FSM, Monastir, 5000, Tunisie.*

^b *University of Lorraine, Laboratoire de Physique et Chimie Théoriques (LPCT), CNRS UMR7019, 54506 Vandoeuvre-Les-Nancy, France.*

Abstract

The effect of the electron-withdrawing fluorine, chlorine, and bromine atoms on the electronic and optical properties of crystalline tetrathienoanthracene and tetrathionoacridine derivatives were investigated by dispersion-corrected density functional theory. Our results also show that the position of sulfur atoms and the substitution of the CH group with a nitrogen atom can improve the charge transport of the title compounds. In addition, slight chemical modifications in the considered molecular derivatives makes smaller the molecular band gaps that facilitates the hole and electron injections. Also the halogenation substituents enhances the hole and the electron transport of the tetrathienoanthracene and tetrathionoacridine compounds. Based on our results, we propose a new set of promising hole and electron transport materials.

Keywords: π -conjugated, Molecular crystal, Chemical modifications, Electronic structure, Optical properties.

1. Introduction

Organic semiconductors (OSCs) are a class of materials that have a wide range of electronic device applications such as organic light-emitting diodes [1, 2, 3, 4, 5], organic field-effect transistors [6, 7, 8, 9, 10, 11, 12], and organic photovoltaic cells [11, 13, 14, 15, 16, 17, 18, 19]. They can produce soft, lightweight, and mechanically flexible materials [20, 21, 22, 23]. The large and the complex design space of conjugated molecules as constituents and their low manufacturing costs, provide a great opportunity for chemical design to achieve diverse physical and chemical properties which make them good alternatives to conventional inorganic semiconductors such as silicon [24, 25, 26].

The development of *n*-type OSCs with high electron mobility has largely lagged behind that of *p*-types ones and still faces the challenge of improving their operational stability due

*I am corresponding author

Email address: saber.gueddida@univ-lorraine.fr (Saber Gueddida)

to the high injection barrier of electrons [27, 28]. On the account of this, a large number of theoretical and experimental works were performed to develop high performance n OSCs [28, 29, 30]. Therefore, developing novel stable and efficient n -type materials is currently a hot and challenging issue. One promising way to convert p to n type OSCs is the functionalization of the p ones by attaching electron-withdrawing substituents such as fluorine, chlorine, or bromine atoms [31, 32, 33, 34, 35]. Attaching electron-withdrawing substituents to π -conjugated ring can lower the energy level of the lowest unoccupied molecular orbital (LUMO) and provide stronger electron affinities, which will facilitate the injection of electrons [29, 30]. Slight chemical modifications of organic molecules such as changing the location of a heteroatom, introducing different substituents and alternative π -conjugated cores are powerful molecular design tools to modulate their optical and electrochemical performance [28, 36, 37, 38].

A wide range of π -conjugated materials (linear arenes, oligothiophenes, and their counterparts) have been studied [39, 40, 41, 42, 43, 44, 45]. The charge carrier mobility in organic materials generally increases with the extension of conjugation. Recently, Liu *et al.* [46] synthesized a new heteroarene compound called tetrathienoanthracene (denoted hereafter TTAn-H) with enhanced π - π stacking and good geometrical stability [36, 47]. An analogous structure with small change in the sulfur positions reported by Brusso *et al.* [32], has shown different optical and electrochemical properties. On the other hand, Robertson and collaborators have shown in recent study [48] that the substitution of the CH group instead of the nitrogen atom in the aromatic core of TTAn-H (called tetrathionoacridine denoted hereafter TTAc-H) reduces the frontier molecular energy levels and the molecular energy band gap. It has been shown that the functionalization of TTAn-H and TTAc-H with fluorine [28] and bromine [47, 37] atoms at the molecular level greatly changes the charge transport, as indicated by X-ray, UV-vis and fluorescence spectroscopy, and scanning tunneling microscopy (STM) studies [32, 47, 48].

Motivated by the interesting fact that a slight chemical modification of organic molecules could induce different optical and electrochemical performance, the aim of this study is to investigate the optical, electronic and transport properties of crystals of TTAn-H and TTAc-H derivatives, and to study the effect of the change in the position of sulfur atoms as well as electron-attracting substituents like fluorine, chlorine and bromine on their properties. In this way, we aim to offer a new set of high-performing n/p type OSCs.

2. Computational details

Molecular and periodic density functional theory calculations were performed using the SIESTA package that uses a basis set of strictly-localized atomic orbitals [49, 50, 51]. The exchange and correlation potential was calculated within the generalized gradient approximation using the Perdew-Burke-Ernzerhof (PBE) formulation [52]. Norm-conserving pseudopotentials of Troullier and Martins in their fully nonlocal form were employed to describe the core electrons [53, 54]. The van der Waals interactions between molecules were included within the Grimme approximation (PBE+D2) as implemented in SIESTA [55].

A double zeta polarization basis set, and an energy cutoff of 120 Ry were used for both TTAn-H and TTAc-H isomers. The Kohn-Sham self-consistent total energy differences were converged within 5×10^{-6} Hartree for both isolated and periodic calculations. Using the Monkhorst-Pack scheme [56], the $2 \times 5 \times 2$ and $2 \times 2 \times 2$ k-points were used in the Brillouin-zone integration for both TTAn-H and TTAc-H derivatives, respectively. In all isolated molecular systems, the periodically repeated molecules were separated by 20 Å of vacuum in all space directions in order to avoid interactions between them. For the atomic relaxation, we relaxed the positions of all the atoms of both isolated and periodic systems by annulling the force on the atoms to within 10^{-5} Ry/Å. The real part of the dielectric function was obtained using the Kramers-Kroning transformation, while the imaginary part is determined by computing the different elements of the dipolar transition matrix between the occupied and the unoccupied states [57].

3. Results and discussions

3.1. Structural Models

The TTAn-H and TTAc-H molecular systems and their substituents with *F*, *Cl*, and *Br* atoms are shown in Figure 1. The TTAn-H molecule contains 36 atoms; 22 carbon, 4 sulfur, and 10 hydrogen atoms. The substitution of the CH group instead of the nitrogen atom in the aromatic core “star-shaped” of TTAn-H molecule leads to the TTAc-H molecule and therefore it contains 35 atoms; 4 sulfur, 21 carbon, 9 hydrogen and one nitrogen atoms. Two molecular isomers for both TTAn-H and TTAc-H are considered in this work: (t-TTAn-H, l-TTAn-H) and (t-TTAc-H, l-TTAc-H), respectively, where the difference between them is the sulfur positions (with $R_1 = R_2 = R_3 = R_4 = H$). For t-TTAn-H or t-TTAc-H, the sulfur atoms are positioned inside, while for l-TTAn-H or l-TTAc-H, they are outside. For each molecular structure, 3 derivatives have been generated by introducing fluorine (denoted hereafter TTAn-F or TTAc-F), chlorine (denoted hereafter TTAn-Cl or TTAc-Cl), and bromine (denoted hereafter TTAn-Br or TTAc-Br) substituents at four positions; ($R_1 = R_2 = R_3 = R_4 = F$), ($R_1 = R_2 = R_3 = R_4 = Cl$), and ($R_1 = R_2 = R_3 = R_4 = Br$), respectively.

After finding the most stable isolated molecular structures for both TTAn-H and TTAc-H and their derivatives, we have optimized their crystal structures using their total energies taking into account the weak van der Waals interactions between the molecules. Figure 2 shows the crystal structures of (t-TTAn-H, l-TTAn-H) and (t-TTAc-H, l-TTAc-H) derivatives, while those of their substituted derivatives are given in the Supporting Information. All the considered systems crystallizes in the monoclinic space group $P2_1/n$. The crystal structure of each derivative contains two stacked π - π molecules in their unit cell slided along the *b* axis, except for the brominated t-TTAn-H and TTAc-H (t-TTAn-Br and TTAc-Br) isomers, which are along *a* and *b* axis (see Figure S1 in the Supporting Information).

Table 1 shows the cell dimensions of the considered derivatives and their equilibrium intermolecular distances (*S-S*, R_i -*S*, R_i - R_i , and π - π with $R_{i=1:4} = F, Cl, \text{ and } Br$). Our results show that the cell parameters are strongly affected by replacing the CH group with a nitrogen atom on the aromatic ring of TTAn-H precursors, and by changing the sulfur

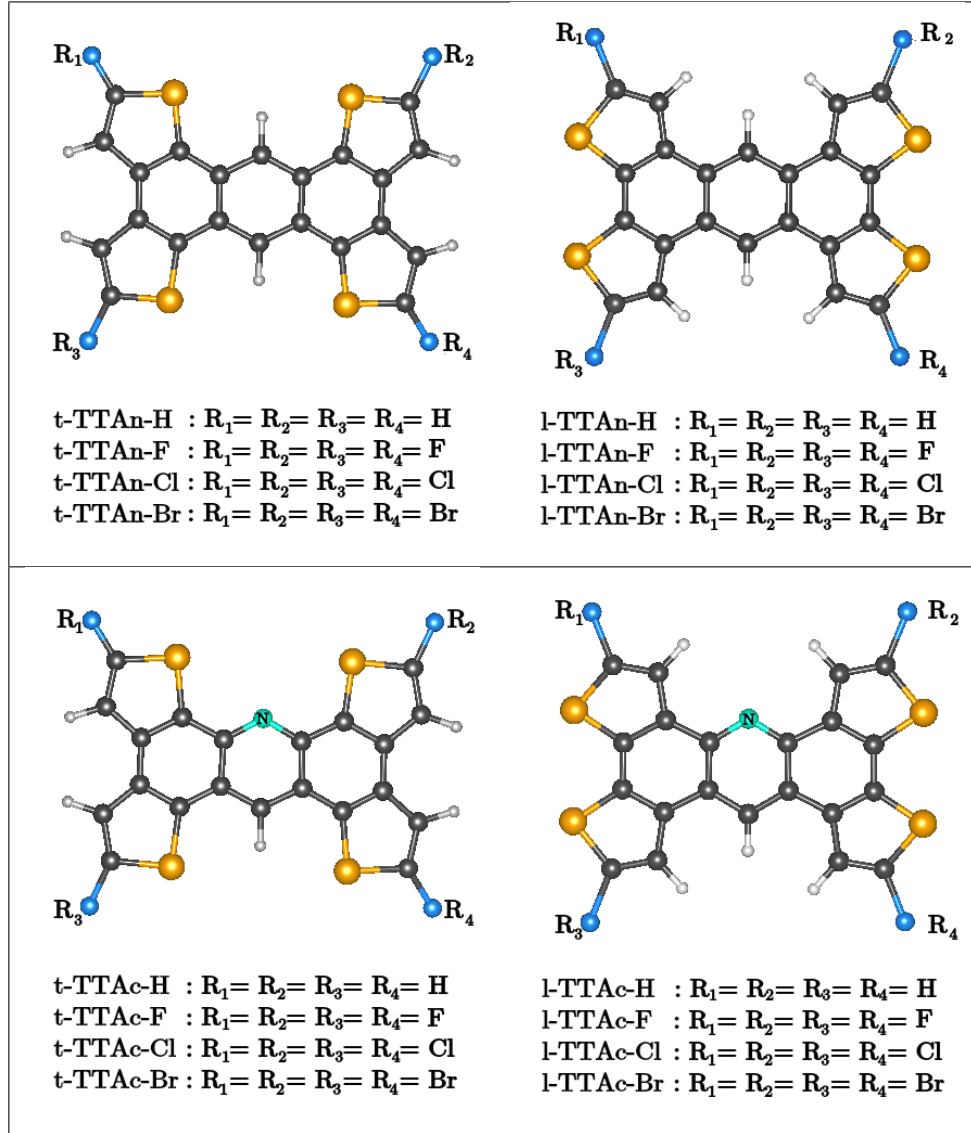


Figure 1: Geometrical structure of the molecular isomers of TTAn-H ($t\text{-TTAn-H}$ and $l\text{-TTAn-H}$) and TTAc-H ($t\text{-TTAc-H}$ and $l\text{-TTAc-H}$) and their substituents with F , Cl and Br atoms: C atoms in dark-gray, S atoms in orange, N atoms in cyan, R_i atoms in blue, and H atoms in white.

positions. The calculated cell parameters for $t\text{-TTAn-H}$ system are in agreement with the experimental results [41] and slightly different for $l\text{-TTAn-H}$ system, while there are no experimental data for the other systems. On the other hand, when the sulfur positions are inside the molecule, we found that the cell parameters are strongly modified by including fluorine, chlorine, and bromine into the TTAn-H and TTAc-H precursors instead of hydrogen atoms which is due probably due to the $F\text{-F}$, $Cl\text{-Cl}$, and $Br\text{-Br}$ intermolecular interactions, while when the sulfur atoms are positioned outside, a slight variation is observed.

The $S\text{-S}$ intermolecular distances are found to be 3.70 Å for both $t\text{-TTAn-H}$ and $l\text{-TTAn-H}$, and 3.66 Å and 3.67 Å for $t\text{-TTAc-H}$ and $l\text{-TTAc-H}$, respectively, with a slight variation of

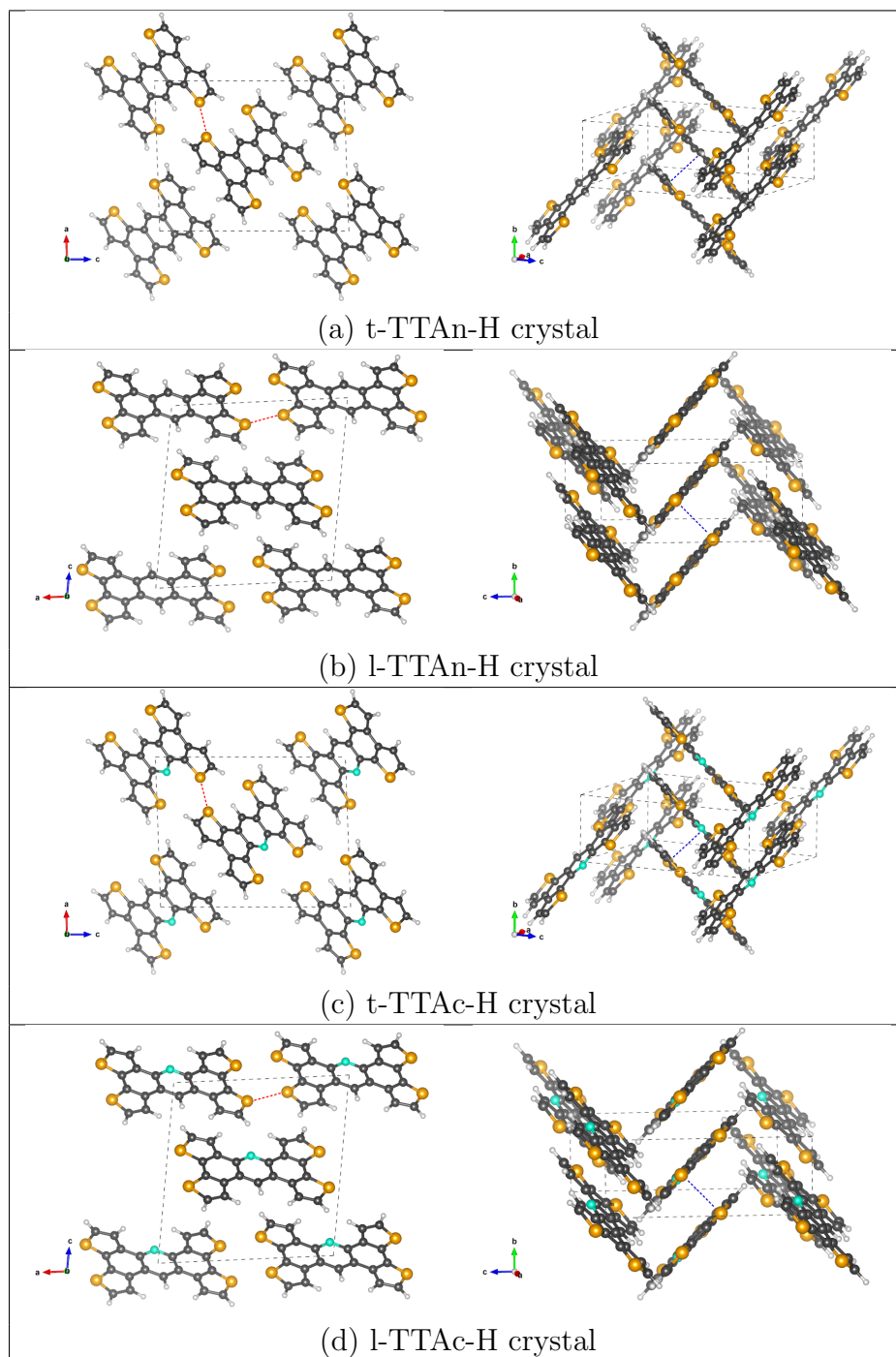


Figure 2: Top and side views of the crystal structure for both TTAn-H (t-TTAn-H: (a), l-TTAn-H: (b)) and TTAc-H (t-TTAc-H: (c), l-TTAc-H: (d)) isomers: C atoms in dark-gray, S atoms in orange, N atoms in cyan, and H atoms in white. The primitive cell of each crystal structure contains 2 molecules. The optimized $S-S$ and $\pi-\pi$ intermolecular distances are shown in red and blue respectively.

Table 1: PBE+D2 calculated crystal cell parameters and equilibrium intermolecular distances (S - S , R - S , R - R , and π - π with $R = F$, Cl , and Br) for the hydrogenation, fluorination, chlorination, and bromination of TTA n and TTA c derivatives. Experimental results when available, are also reported.

	Crystal cell parameters				Intermolecular distances			
	a (Å)	b (Å)	c (Å)	β (°)	S - S (Å)	R - S (Å)	R - R (Å)	π - π (Å)
t-TTA n -H	11.40	5.10	14.34	92.00	3.70	-	-	3.36
Exp ^[41]	11.28	5.03	14.31	92.01	3.77	-	-	3.35
t-TTA n -F	11.47	5.17	14.40	92.02	3.69	2.76	2.88	3.39
t-TTA n -Cl	11.52	5.23	14.55	91.97	3.71	2.78	2.91	3.42
t-TTA n -Br	13.96	3.90	19.98	106.21	3.53	4.33	4.96	3.88
l-TTA n -H	12.05	4.96	12.42	97.58	3.70	-	-	4.78
Exp ^[41]	12.38	5.26	12.80	97.75	3.72	-	-	3.39
l-TTA n -F	12.09	4.97	12.50	97.58	3.71	3.03	2.68	4.79
l-TTA n -Cl	12.15	5.02	12.69	97.69	3.73	3.06	2.69	4.88
l-TTA n -Br	12.23	5.12	12.69	97.75	3.76	3.13	2.75	4.98
t-TTA c -H	11.27	5.03	14.30	92.01	3.66	-	-	3.37
t-TTA c -F	11.32	5.07	14.36	91.99	3.68	2.84	2.88	3.40
t-TTA c -Cl	11.40	5.13	14.42	91.98	3.71	2.86	2.89	3.42
t-TTA c -Br	13.86	3.87	19.98	107.45	3.37	3.86	5.01	3.86
l-TTA c -H	12.00	4.67	12.21	97.48	3.67	-	-	4.53
l-TTA c -F	12.00	4.74	12.50	97.78	3.70	2.98	2.59	4.56
l-TTA c -Cl	12.05	5.00	12.49	97.59	3.72	3.02	2.67	4.84
l-TTA c -Br	12.04	5.08	12.07	97.55	3.74	3.05	2.72	4.04

0.03-0.04 Å due to the replacement of the CH group by a nitrogen atom. These distances are slightly affected by putting fluorine and chlorine instead of the hydrogen atoms. However, for the brominated derivatives for both TTA n -H and TTA c -H, the S - S distances are strongly affected with a value of 3.53 Å and 3.76 Å for t-TTA n -Br and l-TTA n -Br, respectively, and much less for t-TTA c -Br and l-TTA c -Br, 3.37 Å and 3.74 Å, respectively. The intermolecular distances π - π are found to be 3.36 Å and 4.78 Å for t-TTA n -H and l-TTA n -H, respectively, and 3.37 Å and 4.53 Å for TTA c -H isomers. These distances are significantly changed due

to changing the sulfur positions and also by replacing the CH group with a nitrogen atom. Our results show that the π - π intermolecular distances are strongly affected by introducing chlorine and bromine atoms.

Table 1 shows that the intermolecular distances R - R between the different substituents are similar for both TTAn-H and TTAc-H crystalline isomers. However, our calculated results show that these distances are strongly influenced with the modification of the sulfur positions. In particular, the Br - Br distances are found to be 4.96 Å and 2.75 Å for t-TTAn-Br and l-TTAn-Br, respectively. While for t-TTAc-Br and l-TTAc-Br, these distances are equal to 5.01 Å and 2.72 Å, respectively. For the intermolecular interaction R - S , we found that their distances are strongly influenced not only by modifying the sulfur positions, but also by replacing the CH group with a nitrogen atom in the aromatic core of TTAn-H isomers. In particular, the Br - S distances are found to be 4.33 Å for t-TTAn-Br and 3.13 Å for l-TTAn-Br, while for t-TTAc-Br and l-TTAc-Br, are 3.86 Å and 3.05 Å, respectively.

4. Electronic properties

4.1. Density of states (DOSs)

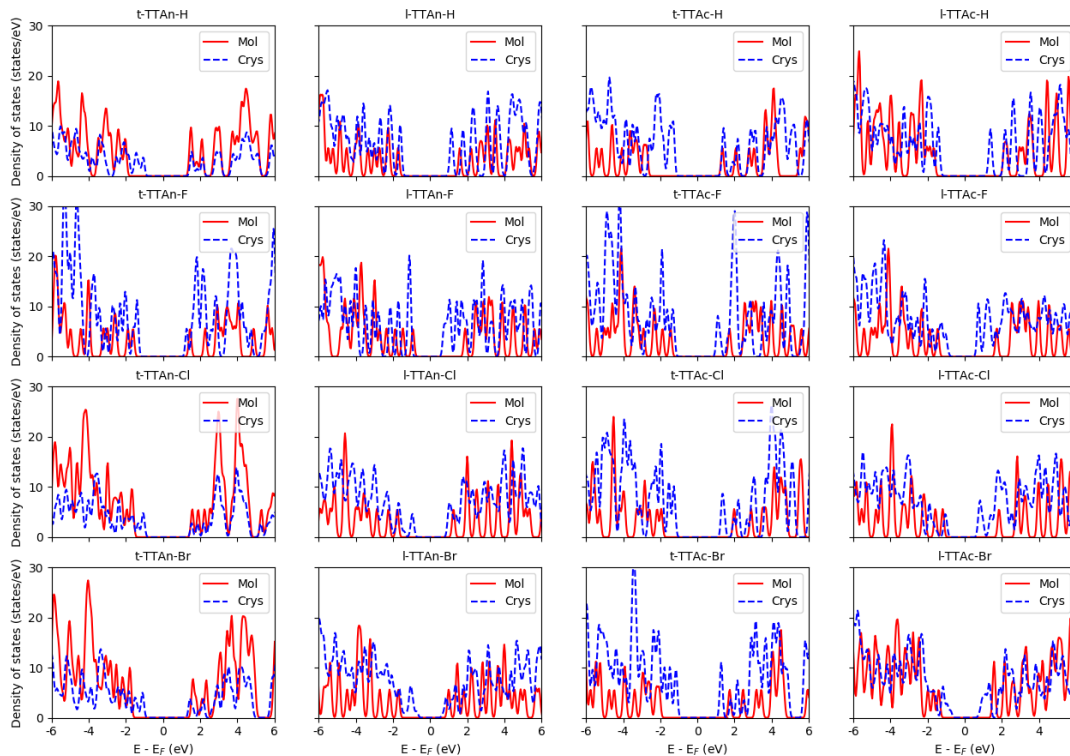


Figure 3: PBE+D2 computed density of states (DOSs) of the isolated and periodic structures (solid red and dashed blue curves, respectively) for both TTAn-H and TTAc-H derivatives (t-TTAn-H, l-TTAn-H, t-TTAc-H, and l-TTAc-H) and their substituents with fluorine, chlorine, and bromine atoms.

Figure 3 shows our computed DOSs for the isolated and molecular structures of TTAn-H and TTAc-H isomers and their fluorinated, chlorinated, and brominated counterparts,

and their band gaps are summarized in Table 2. By comparing the DOSs of the TTAn-H and TTAc-H molecular isomers, we found that the shape and the position of occupied and unoccupied peaks are strongly influenced by replacing the CH group with nitrogen in the aromatic core of TTAn-H, and much less by changing the sulfur positions. The replacement of the CH group with a nitrogen atom shows a shifting of the peaks of the occupied and unoccupied states towards negative and positive energies, respectively. This increases the band gap from 2.87 eV for t-TTAn-H isomer to 3.46 eV for t-TTAc-H one, and from 2.69 eV for l-TTAn-H to 3.19 eV for l-TTAc-H. For both TTAn-H and TTAc-H isomers, our results show a displacement of the peaks of occupied and unoccupied states to positive energies due to the change of the sulfur positions. This result in a reduction of the band gap of about 0.18 eV and 0.27 eV for TTAn-H and TTAc-H isomers, respectively. The calculated molecular band gaps are slightly different from those found in the literature [28, 36, 37], due probably to the different functional used.

Table 2: PBE+D2 calculated band gaps for isolated and periodic structures for the hydrogenation, fluorination, chlorination, and bromination of TTAn and TTAc derivatives (in eV).

Isomers	Isolated	Periodic	Isomers	Isolated	Periodic
t-TTAn-H	2.87	1.94	l-TTAn-H	2.69	2.00
t-TTAn-F	2.47	2.03	l-TTAn-F	2.19	1.20
t-TTAn-Cl	2.60	1.96	l-TTAn-Cl	2.42	1.26
t-TTAn-Br	2.73	1.88	l-TTAn-Br	2.06	0.84
t-TTAc-H	3.46	2.03	l-TTAc-H	3.19	2.05
t-TTAc-F	3.10	1.72	l-TTAc-F	2.56	1.04
t-TTAc-Cl	3.29	1.92	l-TTAc-Cl	2.42	1.09
t-TTAc-Br	3.21	1.76	l-TTAc-Br	2.36	0.92

By comparing the DOSs of the isolated molecular systems, we found that the shape of the occupied and unoccupied peaks is clearly modified by introducing *F*, *Cl*, and *Br* at four positions into the TTAn-H and TTAc-H precursors. A displacement towards the higher energies of the occupied states is noticed for the substituted derivatives of both t-TTAn-H and t-TTAc-H precursors, while for those of l-TTAn-H and l-TTAc-H, the occupied and unoccupied peaks are moved towards the Fermi level with respect to those of the precursors ones. This reduces strongly the band gaps of the substituted l-TTAn-H and l-TTAc-H derivatives, and much less for those of t-TTAn-H and t-TTAc-H ones. The band gaps are of 2.47, 2.60, and 2.73 eV for t-TTAn-F, t-TTAn-Cl, and t-TTAn-Br, respectively, and 2.19, 2.42, and 2.06 eV for l-TTAn-F, l-TTAn-Cl, and l-TTAn-Br, respectively. The band gaps of t-TTAc-F, t-TTAc-Cl, and t-TTAc-Br are of 3.10, 3.29, and 3.21 eV, respectively, while

those of the substituted derivatives of l-TTAc-H, are 2.56, 2.42, and 2.36 eV. We found that the modification of the sulfur positions and the substitution of the CH group with a nitrogen atom have a strong effect on the molecular band gaps.

For the crystal structures of the four derivatives (t-TTAn-H, l-TTAn-H, t-TTAc-H, and l-TTAc-H), most of the peaks of the occupied and unoccupied states are broadened. For t-TTAn-H and t-TTAc-H crystals, the peaks mostly of the occupied states are displaced to the Fermi level, while for l-TTAn-H and l-TTAc-H, both the occupied and the unoccupied peaks are shifted. Therefore, we found that the band gaps of the periodic structures are reduced compared to those of the isolated ones due to the intermolecular interactions between sulfur atoms. The band gaps of t-TTAn-H and l-TTAn-H crystals are found to be 1.94 and 2.00 eV, respectively, while for t-TTAc-H and l-TTAc-H, are 2.03 and 2.05 eV, respectively.

The substitution of hydrogen by fluorine, chlorine, and bromine atoms shows also that most of the occupied and unoccupied peaks are broadened and displaced towards the Fermi level that depend not only on the sulfur sites but also on the *F-F*, *Cl-Cl*, and *Br-Br* intermolecular interactions. This reduces the band gaps to 2.03, 1.96, and 1.88 eV for t-TTAn-F, t-TTAn-Cl, and t-TTAn-Br, respectively, while for the substituted derivatives of l-TTAn-H, they are 1.20, 1.26, and 0.84 eV, respectively. For fluorination, chlorination, and bromination of the precursor t-TTAc-H, the band gaps are found to be 1.72, 1.92, and 1.76 eV, respectively, while those of the precursors l-TTAc-H, are 1.04, 1.09 eV, and 0.92 eV. We found that the band gaps of the crystalline structures are strongly affected where the sulfur atoms exposed outside which increases the *S-S* interactions. For both TTAn-H and TTAc-H derivatives, the bromination has stronger effects compared to that of fluorination and chlorination and leads to smaller band gaps. Our results show that changing the sulfur positions, replacing the CH group with a nitrogen atom in the aromatic core of TTAn-H, and the electronic properties, in particular the DOSs, are influenced by introducing *F*, *Cl*, and *Br* instead of hydrogen atoms. We conclude that the chemical modification in TTAn-H and TTAc-H systems reduces the band gaps, which facilitates electron/hole injection.

We have plotted also the projected DOSs curves (see Figure S4 in the Supporting Information) for the two most representative isomers (l-TTAn-Br and l-TTAc-Br) to indicate the predominant contributions of the electronic states in the different regions of the valence band and the conduction band. For the molecular structures, our results show that the top of the valence band consists of the contribution mainly of carbon and bromine atoms for both l-TTAn-Br and l-TTAc-Br systems, while for the bottom of the conduction band is the contribution of carbon and sulfur atoms for l-TTAn-Br, and carbon and bromine atoms for l-TTAc-Br. For the crystal structures, we found that mainly electronic states associated with carbon and bromine atoms contribute to the top valence band, while the bottom of the conduction band consists of electronic state contributions of carbon, bromine and sulfur atoms.

4.2. Band structure

In general, the anisotropy in the electron and/or hole transport of such material can be understood qualitatively by the appearance of either flat or dispersive bands. A significant charge (electron/hole) carrier mobility is related to a large (conduction/valence) band, while

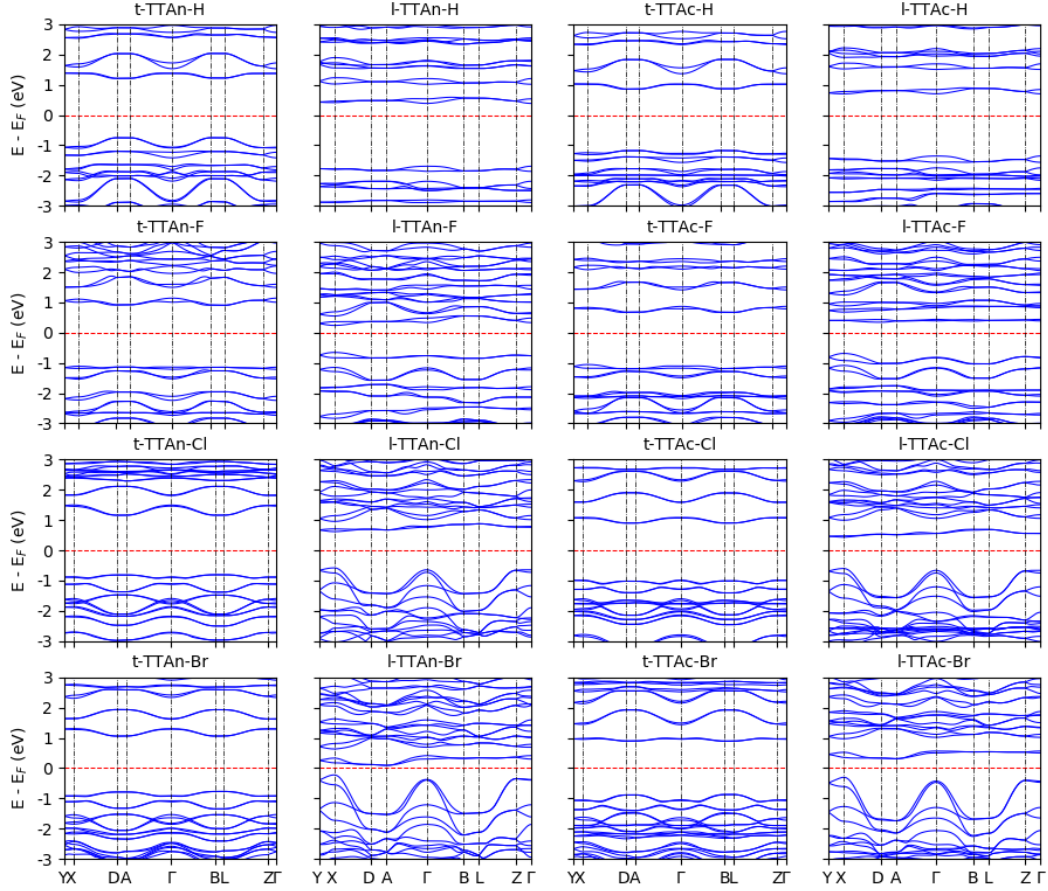


Figure 4: PBE+D2 calculated band structure of crystal isomers of TTAn-H and TTAc-H and their fluorinated, chlorinated, and brominated derivatives.

a low mobility correlates with relatively a flat band [28, 36]. Figure 4 shows the computed band structures of t-TTAn-H, l-TTAn-H, t-TTAc-H, and l-TTAc-H crystals and their derivatives. Because the primitive unit cell of all considered derivatives contains two inequivalent organic molecules, the conduction and the valence bands are doubly degenerated.

Our results show that both conduction and valence bands of t-TTAn-H are strongly dispersive along the directions XD , ΓA and ΓB . We clearly observe that the valence bands are larger than the conduction bands, which signifies that the holes mobility is greater than the one of electrons, and therefore t-TTAn-H can act as a two-dimensional (2D) hole transport material. For l-TTAn-H, the flat conduction and valence bands in all directions suggesting very low electron and hole mobilities with respect to those of the t-TTAn-H crystal. We conclude that the Sulfur-Sulfur interactions increased by modifying the sulfur positions, plays a useful role in controlling the charge carrier transport. The substitution of the CH group instead of the nitrogen atom in the aromatic core of t-TTAn-H reduces the hole carrier mobility, and therefore the t-TTAc-H is an electron transport material. However, the hole and electron transport properties of l-TTAc-H are not affected by this replacement

in l-TTAn-H. We found that t-TTAn-H and t-TTAc-H are direct bandgap semiconductors. Our results show that the replacement of CH group has significant effect on charge carrier transport only where the sulfur atoms are positioned inside.

On the other hand, our results show that the introduction of bromine atoms enhances the electron and hole mobility of the t-TTAn-H and t-TTAc-H precursors, respectively. This suggest that t-TTAn-Br can act as an electron transport material, while t-TTAc-Br is a hole transport one. We found that the chlorination of the t-TTAn-H and t-TTAc-H precursors improves the electron transport of these systems. In addition, the chlorinated substituent of t-TTAc-H shows an improvement in the dispersion of the valence band in all directions. However, by introducing chlorine or bromine atoms into the l-TTAn-H and l-TTAc-H precursors instead of the hydrogen atoms, our calculations show a large dispersion of the valence band in different directions and therefore very high hole mobilities.

For t-TTAn-F, l-TTAn-F, and t-TTAc-F, the large conduction bands in all directions suggests high electron mobilities, and that these crystals are electron organic materials. The flat valence band of these materials in all directions suggests very low hole mobilities compared with those of t-TTAn-H, l-TTAn-H, and t-TTAc-H. However, the fluorinated derivative of l-TTAc-H shows a large dispersion of the valence band while the conduction band is a flat, which indicates that l-TTAc-F can act as hole transport material.

We therefore deduce that the fluorine, chlorine, and bromine atoms introduced into the TTAn-H and TTAc-H derivatives instead of the hydrogen atoms are very useful to control the charge carrier transport. In particular, a large dispersive valence band in different directions is observed by introducing the chlorine and bromine substituents in l-TTAn-H and l-TTAc-H precursors, which is also characteristic of a number of chlorine- and bromine-bearing crystals such as TlPb_2Br_5 [58], TlPb_2Cl_5 [59], and Tl_3PbBr_5 [60]. On the other hand, we found that the substitution of the CH group instead of the nitrogen atom in the aromatic ring of TTAn-H precursors does not affect strongly the transport properties. To conclude, our results show that t-TTAn-H, l-TTAn-Cl, l-TTAn-Br, t-TTAc-Br, l-TTAc-F, l-TTAc-Cl, and l-TTAc-Br are promising hole transport materials, while, t-TTAn-F, t-TTAn-Cl, t-TTAn-Br, l-TTAn-F, t-TTAc-H, t-TTAc-F, and t-TTAc-Cl are promising electron transport materials.

4.3. Optical properties

For such systems, the optical absorption properties are generally investigated by computing the complex dielectric function:

$$\varepsilon(\omega) = \varepsilon_1(\omega) + i\varepsilon_2(\omega), \quad (1)$$

where ω is the frequency and $\varepsilon_1(\omega)$ and $\varepsilon_2(\omega)$ represent its real and imaginary parts, respectively. Figure 5 shows the computed real and imaginary parts of the dielectric function with energy. The static values of the real part of the dielectric function at $\omega = 0$ for the hydrogenation, fluorination, chlorination, and bromination of TTAn and TTAc crystalline isomers are summarized in Table 3.

According to the calculated values of $\varepsilon_1(0)$ of t-TTAn-H, l-TTAn-H, t-TTAc-H, and l-TTAc-H derivatives in Table 3, we found that t-TTAc-H has the largest $\varepsilon_1(0)$ and therefore

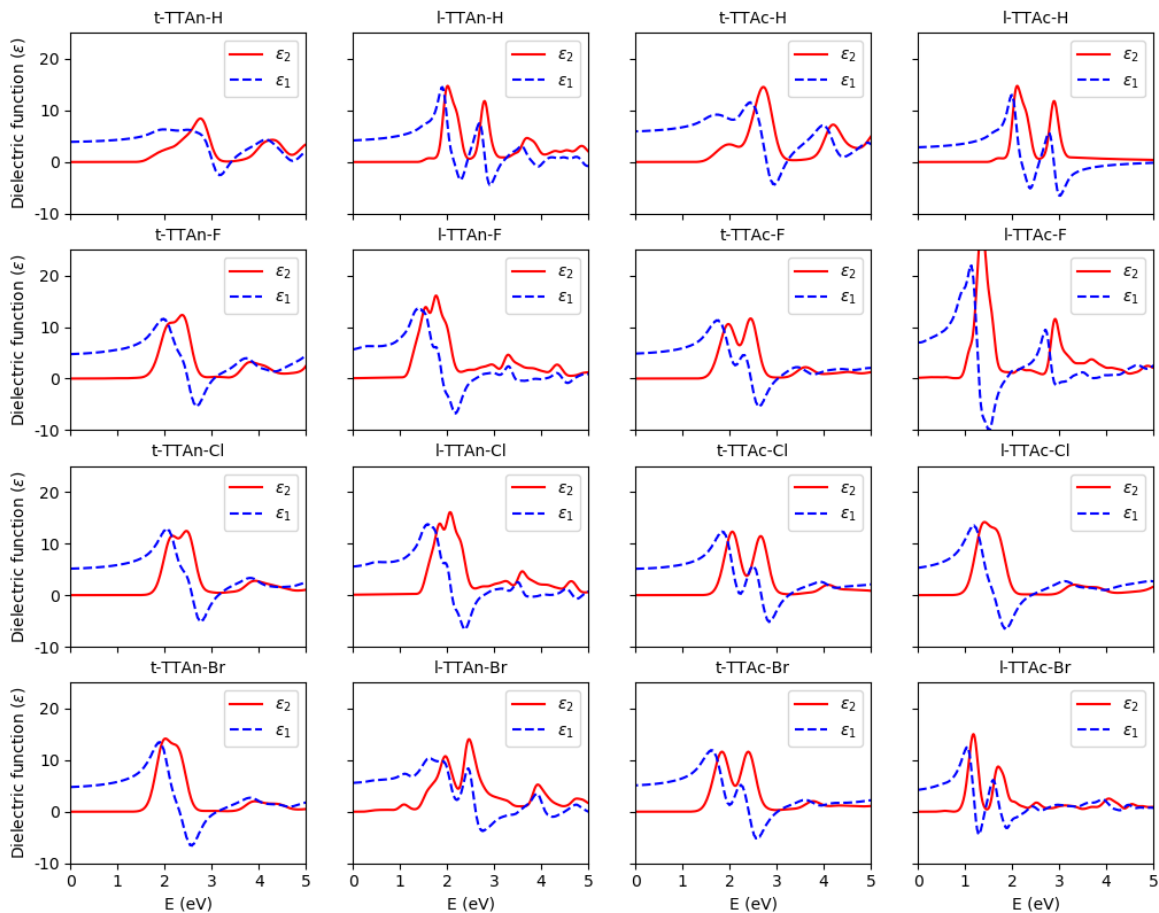


Figure 5: PBE+D2 calculated $\epsilon_1(\omega)$ (dashed blue curve) and $\epsilon_2(\omega)$ (solid red curve) as a function of total energy in eV for the hydrogenation, fluorination, chlorination, and bromination of TTAn and TTAc derivatives.

it shows the best optical screening, while l-TTAc-H has the lowest value and therefore it has the poorest one. The static dielectric constant $\epsilon_1(0)$ of t-TTAn-H, l-TTAn-H, t-TTAc-H, and l-TTAc-H isomers are found to be 3.90, 4.18, 5.94, and 2.68, respectively. The calculated results show that the sulfur positions and the introduction of the CH group instead of a nitrogen atom influences the optical properties.

The fluorination, chlorination, and bromination of both TTAn-H and TTAc-H derivatives show good optical response. In all cases, attaching electron-withdrawing substituents to the TTAn-H and TTAc-H isomers increases $\epsilon_1(0)$, except for the substituted derivatives of t-TTAc-H, it decreases compared to the precursor one but it remains higher compared to the other compounds. The static dielectric constant $\epsilon_1(0)$ of t-TTAn-F, t-TTAn-Cl, and t-TTAn-Br are found to be 4.73, 5.13, and 4.77, respectively, while for l-TTAn-H derivatives, are 5.67, 5.52, and 5.58. For t-TTAc-H derivatives, the $\epsilon_1(0)$ are found to be 4.85, 5.10, and 5.11 eV by replacing hydrogen with fluorine, chlorine, and bromine atoms, respectively, while those of the l-TTAc-H derivatives, are 7.00, 5.28, and 4.22, respectively. Our results

Table 3: PBE+D2 computed $\varepsilon_1(0)$ for the hydrogenation, fluorination, chlorination, and bromination of TTAn and TTAc derivatives.

Systems	$\varepsilon_1(0)$	Systems	$\varepsilon_1(0)$
t-TTAn-H	3.90	l-TTAn-H	4.18
t-TTAn-F	4.73	l-TTAn-F	5.67
t-TTAn-Cl	5.13	l-TTAn-Cl	5.52
t-TTAn-Br	4.77	l-TTAn-Br	5.58
t-TTAc-H	5.94	l-TTAc-H	2.68
t-TTAc-F	4.85	l-TTAc-F	7.00
t-TTAc-Cl	5.10	l-TTAc-Cl	5.28
t-TTAc-Br	5.11	l-TTAc-Br	4.22

show that l-TTAc-F has the best optical response.

The variation of $\varepsilon_1(\omega)$ and $\varepsilon_2(\omega)$ (see Figure 5) shows mainly two peaks for all derivatives, where the two peaks of the imaginary part. $\varepsilon_1(\omega)$ shows oscillations up to 3.5 eV, then all curves merge and the optical response becomes very low. On the other hand, it is shown that for the best optical response, by replacing the hydrogen atoms with fluorine and bromine into the TTP systems, the peaks of $\varepsilon_1(\omega)$ and $\varepsilon_2(\omega)$ are shifted towards lower energies with respect to those of the precursor ones, while when they are shifted towards higher energies, the optical response is weak. In this work, by introducing fluorine, chlorine, and bromine into both TTAn-H and TTAc-H derivatives instead of hydrogen atoms, we found that the peaks of the real and the imaginary parts of the dielectric function are shifted to lower energies as compared to those of the precursor ones, and therefore they have good optical response. Our results show that the most optimal optical response are obtained with the following systems: t-TTAn-H, t-TTAn-F, t-TTAn-Cl, t-TTAn-Br, l-TTAn-F, l-TTAn-Cl, l-TTAn-Br, t-TTAc-H, t-TTAc-F, t-TTAc-Cl, t-TTAc-Br, l-TTAc-F, l-TTAc-Cl, and l-TTAc-Br. The optical absorption properties are consistent with the results obtained in the electronic part (DOSs and band structure).

5. Conclusions

The electronic and optical properties of crystalline structures of the hydrogenation, fluorination, chlorination, and bromination of tetrathienoanthracene and tetrathioacridine derivatives are predicted by means of density functional theory. We have analyzed how the position of the sulfur atoms, the replacement of the CH group with nitrogen and fluorination, chlorination, and bromination change the transport properties in TTAn-H and TTAc-H derivatives. Our results show that the chemical modifications in TTAn-H and

TTAc-H molecular derivatives reduces the gaps, which facilitate the hole and the electron injections. We found that the location of the sulfur atoms has a strong effect on the band gap of the crystalline structures. Also we showed that the replacement of fluorine, chlorine, and bromine instead of the hydrogen atoms enhances the hole/electron transport of the TTAn-H and TTAc-H precursors. Moreover, the chlorination and bromination of l-TTAn-H and l-TTAc-H give rise to a large dispersing valence band in different directions and therefore a very high hole mobility. The calculated band structures indicate that t-TTAn-H, l-TTAn-Cl, l-TTAn-Br, t-TTAc-Br, l-TTAc-F, l-TTAc-Cl, and l-TTAc-Br are promising hole transport materials, while, t-TTAn-F, t-TTAn-Cl, t-TTAn-Br, l-TTAn-F, t-TTAc-H, t-TTAc-F, and t-TTAc-Cl are promising electron transport materials. The computed dielectric functions confirm that the most optimal optical response are obtained with the following systems: t-TTAn-H, t-TTAn-F, t-TTAn-Cl, t-TTAn-Br, l-TTAn-F, l-TTAn-Cl, l-TTAn-Br, t-TTAc-H, t-TTAc-F, t-TTAc-Cl, t-TTAc-Br, l-TTAc-F, l-TTAc-Cl, and l-TTAc-Br.

Acknowledgment

We acknowledge useful advice and insight provided by Dietrich Foerster.

Data Availability

The data that support the findings of this study are available from the corresponding author upon reasonable request.

References

- [1] E. Williams, K. Haavisto, J. Li, G. Jabbour, Excimer-based white phosphorescent organic light-emitting diodes with nearly 100% internal quantum efficiency, *Adv. Mater.* 19 (2) (2007) 197–202. doi:10.1002/adma.200602174.
- [2] J. Huang, J.-H. Su, H. Tian, The development of anthracene derivatives for organic light-emitting diodes, *J. Mater. Chem.* 22 (2012) 10977–10989. doi:10.1039/C2JM16855C.
- [3] G. Gigli, G. Barbarella, L. Favaretto, F. Cacialli, R. Cingolani, High-efficiency oligothiophene-based light-emitting diodes, *Appl. Phys. Lett.* 75 (4) (1999) 439–441. doi:10.1063/1.124403.
- [4] H. J. Baek, S. E. Lee, H. W. Lee, J. Kang, J. Park, S. S. Yoon, Y. K. Kim, Efficient co-host exciplex emission for white organic light-emitting diodes, *J. Phys. Chem. Solids* 119 (2018) 276 – 280. doi:https://doi.org/10.1016/j.jpcs.2018.03.016.
- [5] D. Shin, K.-Y. Hong, J. Park, Effect of pre-drying treatments on solution-coated organic thin films for active-matrix organic light-emitting diodes, *J. Phys. Chem. Solids* 111 (2017) 18 – 24. doi:https://doi.org/10.1016/j.jpcs.2017.07.016.
- [6] Y. Qiao, Y. Guo, C. Yu, F. Zhang, W. Xu, Y. Liu, D. Zhu, Diketopyrrolopyrrole-containing quinoidal small molecules for high-performance, air-stable, and solution-processable n-channel organic field-effect transistors, *J. Am. Chem. Soc.* 134 (9) (2012) 4084–4087. doi:10.1021/ja3003183.
- [7] R. P. Ortiz, J. Casado, V. Hernandez, J. L. Navarrete, J. Letizia, M. Ratner, A. Facchetti, T. Marks, Thiophene-diazine molecular semiconductors: Synthesis, structural, electrochemical, optical, and electronic structural properties; implementation in organic field-effect transistors, *Chem.-Eur. J.* 15 (20) (2009) 5023–5039. doi:10.1002/chem.200802424.
- [8] Y. Geng, H.-B. Li, S.-X. Wu, Z.-M. Su, The interplay of intermolecular interactions, packing motifs and electron transport properties in perylene diimide related materials: a theoretical perspective, *J. Mater. Chem.* 22 (2012) 20840–20851. doi:10.1039/C2JM33369D.

- [9] D. T. Chase, A. G. Fix, S. J. Kang, B. D. Rose, C. D. Weber, Y. Zhong, L. N. Zakharov, M. C. Lonergan, C. Nuckolls, M. M. Haley, 6,12-diarylindeno[1,2-b]fluorenes: Syntheses, photophysics, and ambipolar OFETs, *J. Am. Chem. Soc.* 134 (25) (2012) 10349–10352. doi:10.1021/ja303402p.
- [10] G. Generali, F. Dinelli, R. Capelli, S. Toffanin, F. di Maria, M. Gazzano, G. Barbarella, M. Muccini, Correlation among morphology, crystallinity, and charge mobility in OFETs made of quaterthiophene alkyl derivatives on a transparent substrate platform, *J. Phys. Chem. C* 115 (46) (2011) 23164–23169. doi:10.1021/jp2090704.
- [11] I. Osaka, T. Abe, M. Shimawaki, T. Koganezawa, K. Takimiya, Naphthodithiophene-based donor-acceptor polymers: Versatile semiconductors for OFETs and OPVs, *ACS Macro Letters* 1 (4) (2012) 437–440. doi:10.1021/mz300065t.
- [12] S. Fratini, A. Morpurgo, S. Ciuchi, Electron-phonon and electron-electron interactions in organic field effect transistors, *J. Phys. Chem. Solids* 69 (9) (2008) 2195 – 2198, study of Matter Under Extreme Conditions 2007. doi:https://doi.org/10.1016/j.jpcs.2008.03.039.
- [13] Y. Lin, Y. Li, X. Zhan, Small molecule semiconductors for high-efficiency organic photovoltaics, *Chem. Soc. Rev.* 41 (2012) 4245–4272. doi:10.1039/C2CS15313K.
- [14] Y.-A. Duan, Y. Geng, H.-B. Li, J.-L. Jin, Y. Wu, Z.-M. Su, Theoretical characterization and design of small molecule donor material containing naphthodithiophene central unit for efficient organic solar cells, *J. Comput. Chem.* 34 (19) (2013) 1611–1619. doi:10.1002/jcc.23298.
- [15] M. S. Park, J. Y. Lee, Indolo acridine-based hole-transport materials for phosphorescent OLEDs with over 20% external quantum efficiency in deep blue and green, *Chem. Mater.* 23 (19) (2011) 4338–4343. doi:10.1021/cm201634w.
- [16] N. Lin, J. Qiao, L. Duan, H. Li, L. Wang, Y. Qiu, Achilles heels of phosphine oxide materials for OLEDs: chemical stability and degradation mechanism of a bipolar phosphine oxide/carbazole hybrid host material, *J. Phys. Chem. C* 116 (36) (2012) 19451–19457. doi:10.1021/jp305415x.
- [17] Z. El Jouad, E. El-Menyawy, G. Louarn, L. Arzel, M. Morsli, M. Addou, J. Bernède, L. Cattin, The effect of the band structure on the voc value of ternary planar heterojunction organic solar cells based on pentacene, boron subphthalocyanine chloride and different electron acceptors, *J. Phys. Chem. Solids* 136 (2020) 109142. doi:https://doi.org/10.1016/j.jpcs.2019.109142.
- [18] S. Ghomrasni, S. Ayachi, K. Alimi, New acceptor-donor-acceptor (A-D-A) type copolymers for efficient organic photovoltaic devices, *J. Phys. Chem. Solids* 76 (2015) 105 – 111. doi:https://doi.org/10.1016/j.jpcs.2014.08.013.
- [19] S. O. Oseni, G. T. Mola, Effects of metal-decorated nanocomposite on inverted thin film organic solar cell, *J. Phys. Chem. Solids* 130 (2019) 120 – 126. doi:https://doi.org/10.1016/j.jpcs.2019.02.015.
- [20] Y. Ie, T. Uto, N. Yamamoto, Y. Aso, Dendritic oligothiophene bearing perylene bis(dicarboximide) groups as an active material for photovoltaic device, *Chem. Commun.* (2009) 1213–1215doi:10.1039/B819008A.
- [21] M. L. Tang, T. Okamoto, Z. Bao, High-performance organic semiconductors: asymmetric linear acenes containing sulphur, *J. Am. Chem. Soc.* 128 (50) (2006) 16002–16003. doi:10.1021/ja066824j.
- [22] L.-L. Chua, J. Zaunseil, J.-F. Chang, E. C.-W. Ou, P. K.-H. Ho, H. Siringhaus, R. H. Friend, General observation of n-type field-effect behaviour in organic semiconductors, *Nature* 434 (2005) 194–199. doi:https://doi.org/10.1038/nature03376.
- [23] L. Jiang, W. Hu, Z. Wei, W. Xu, H. Meng, High-performance organic single-crystal transistors and digital inverters of an anthracene derivative, *Adv. Mater.* 21 (36) (2009) 3649–3653. doi:10.1002/adma.200900503.
- [24] Y.-A. Forrest, The path to ubiquitous and low-cost organic electronic appliances on plastic, *Nature* 428 (2004) 911–918. doi:https://doi.org/10.1038/nature02498.
- [25] M. Mas-Torrent, C. Rovira, Role of molecular order and solid-state structure in organic field-effect transistors, *Chem. Rev.* 111 (8) (2011) 4833–4856. doi:10.1021/cr100142w.
- [26] K. Hummer, C. Ambrosch-Draxl, Electronic properties of oligoacenes from first principles, *Phys. Rev. B* 72 (2005) 205205. doi:10.1103/PhysRevB.72.205205.
- [27] P. F. Baude, D. A. Ender, M. A. Haase, T. W. Kelley, D. V. Muyres, S. D. Theiss,

- Pentacene-based radio-frequency identification circuitry, *Appl. Phys. Lett.* 82 (22) (2003) 3964–3966. doi:10.1063/1.1579554.
- [28] J. Yin, K. Chaitanya, X.-H. Ju, Theoretical investigation of fluorination effect on the charge carrier transport properties of fused anthra-tetrathioephene and its derivatives, *J. Mol. Graph. Model.* 64 (2016) 40 – 50. doi:https://doi.org/10.1016/j.jmgm.2015.12.007.
- [29] J. C. Sancho-Garcia, A. J. Perez-Jimenez, Y. Olivier, J. Cornil, Molecular packing and charge transport parameters in crystalline organic semiconductors from first-principles calculations, *Phys. Chem. Chem. Phys.* 12 (2010) 9381–9388. doi:10.1039/B925652K.
- [30] S. Chai, S.-H. Wen, J.-D. Huang, K.-L. Han, Density functional theory study on electron and hole transport properties of organic pentacene derivatives with electron-withdrawing substituent, *J. Comput. Chem.* 32 (15) (2011) 3218–3225. doi:10.1002/jcc.21904.
- [31] W. Wu, Y. Liu, D. Zhu, π -conjugated molecules with fused rings for organic field-effect transistors: design, synthesis and applications, *Chem. Soc. Rev.* 39 (2010) 1489–1502. doi:10.1039/B813123F.
- [32] J. L. Brusso, O. D. Hirst, A. Dadvand, S. Ganesan, F. Cicoira, C. M. Robertson, R. T. Oakley, F. Rosei, D. F. Perepichka, Two-dimensional structural motif in thienoacene semiconductors: Synthesis, structure, and properties of tetrathienoanthracene isomers, *Chem. Mater.* 20 (7) (2008) 2484–2494. doi:10.1021/cm7030653.
- [33] C. Roger, F. Wurthner, Core-tetrasubstituted naphthalene diimides: synthesis, optical properties, and redox characteristics, *J. Org. Chem.* 72 (21) (2007) 8070–8075. doi:10.1021/jo7015357.
- [34] S. A. Sharber, S. W. Thomas, Side chain regioisomers that dictate optical properties and mechanofluorochromism through crystal packing, *Chem. Mater.* 32 (13) (2020) 5785–5801. doi:10.1021/acs.chemmater.0c01676.
- [35] H. Bouazizi, A. Mabrouk, M. Braïek, T. Mestiri, K. Alimi, New conjugated organic matrix-carbon nanotube functionalization: DFT modeling and spectroscopic analysis, *J. Phys. Chem. Solids* 136 (2020) 109131. doi:https://doi.org/10.1016/j.jpcs.2019.109131.
- [36] Y.-A. Duan, H.-B. Li, Y. Geng, Y. Wu, G.-Y. Wang, Z.-M. Su, Theoretical studies on the hole transport property of tetrathienoarene derivatives: The influence of the position of sulfur atom, substituent and π -conjugated core, *Org. Electron.* 15 (2) (2014) 602 – 613. doi:https://doi.org/10.1016/j.orgel.2013.12.011.
- [37] J. Yin, X.-H. Chaitanya, Kadaliand Ju, Bromination and cyanation for improving electron transport performance of anthra-tetrathioephene, *J. Mater. Res.* 31 (2016) 337–347. doi:10.1557/jmr.2016.8.
- [38] P. Cudazzo, F. Sottile, A. Rubio, M. Gatti, Exciton dispersion in molecular solids, *J. Phys.: Condens. Matter* 27 (11) (2015) 113204. doi:10.1088/0953-8984/27/11/113204.
- [39] C. Reese, M. Roberts, M. mang Ling, Z. Bao, Organic thin film transistors, *Mater. Today* 7 (9) (2004) 20 – 27. doi:https://doi.org/10.1016/S1369-7021(04)00398-0.
- [40] C. Dimitrakopoulos, P. Malenfant, Organic thin film transistors for large area electronics, *Adv. Mater.* 14 (2) (2002) 99–117. doi:10.1002/1521-4095(20020116).
- [41] A. Facchetti, M.-H. Yoon, C. L. Stern, G. R. Hutchison, M. A. Ratner, T. J. Marks, Building blocks for n-type molecular and polymeric electronics. perfluoroalkyl- versus alkyl-functionalized oligothiophenes (nts; n = 2-6). systematic synthesis, spectroscopy, electrochemistry, and solid-state organization, *J. Am. Chem. Soc.* 126 (41) (2004) 13480–13501. doi:10.1021/ja048988a.
- [42] Z. Wang, C. Kim, A. Facchetti, T. J. Marks, Anthracenedicarboximides as air-stable n-channel semiconductors for thin-film transistors with remarkable current on/off ratios, *J. Am. Chem. Soc.* 129 (44) (2007) 13362–13363. doi:10.1021/ja073306f.
- [43] H. Meng, F. Sun, M. B. Goldfinger, G. D. Jaycox, Z. Li, W. J. Marshall, G. S. Blackman, High-performance, stable organic thin-film field-effect transistors based on bis-5'-alkylthiophen-2'-yl-2,6-anthracene semiconductors, *J. Am. Chem. Soc.* 127 (8) (2005) 2406–2407. doi:10.1021/ja043189d.
- [44] A. Mishra, C.-Q. Ma, P. Bauerle, Functional oligothiophenes: Molecular design for multidimensional nanoarchitectures and their applications, *Chem. Rev.* 109 (3) (2009) 1141–1276. doi:10.1021/cr8004229.
- [45] X.-D. Tang, Y. Liao, H. Geng, Z.-G. Shuai, Fascinating effect of dehydrogenation on the transport properties of n-heteropentacenes: transformation from p- to n-type semiconductor, *J. Mater. Chem.* 22 (2012) 18181–18191. doi:10.1039/C2JM33039C.

- [46] L. Liu, G. Yang, Y. Duan, Y. Geng, Y. Wu, Z. Su, The relationship between intermolecular interactions and charge transport properties of trifluoromethylated polycyclic aromatic hydrocarbons, *Org. Electron.* 15 (9) (2014) 1896 – 1905. doi:<https://doi.org/10.1016/j.orgel.2014.05.020>.
- [47] A. A. Leitch, A. Mansour, K. A. Stobo, I. Korobkov, J. L. Brusso, Functionalized tetrathienoanthracene: Enhancing π - π interactions through expansion of the π -conjugated framework, *Cryst. Growth & Des.* 12 (3) (2012) 1416–1421. doi:10.1021/cg201521w.
- [48] S. Robertson, A. Leitch, I. Korobkov, D. Soldatov, J. Brusso, Functionalized thienoacridines: synthesis, optoelectronic, and structural properties, *Can. J. Chem.* 92 (2014) 1106–1110. doi:10.1139/cjc-2014-0348.
- [49] W. Kohn, L. J. Sham, Self-consistent equations including exchange and correlation effects, *Phys. Rev.* 140 (1965) A1133–A1138. doi:10.1103/PhysRev.140.A1133.
- [50] J. M. Soler, E. Artacho, J. D. Gale, A. García, J. Junquera, P. Ordejón, D. Sánchez-Portal, The SIESTA method for ab initio order-n materials simulation, *J. Phys.: Condens. Matter* 14 (11) (2002) 2745–2779. doi:10.1088/0953-8984/14/11/302.
- [51] D. Sánchez-Portal, P. Ordejón, E. Artacho, J. M. Soler, Density-functional method for very large systems with LCAO basis sets, *Int. J. Quantum Chem.* 65 (5) (1997) 453–461. doi:10.1002/(SICI)1097-461X(1997).
- [52] J. P. Perdew, K. Burke, M. Ernzerhof, Generalized gradient approximation made simple, *Phys. Rev. Lett.* 77 (1996) 3865–3868. doi:10.1103/PhysRevLett.77.3865.
- [53] N. Troullier, J. L. Martins, Efficient pseudopotentials for plane-wave calculations, *Phys. Rev. B* 43 (1991) 1993–2006. doi:10.1103/PhysRevB.43.1993.
- [54] L. Kleinman, D. M. Bylander, Efficacious form for model pseudopotentials, *Phys. Rev. Lett.* 48 (1982) 1425–1428. doi:10.1103/PhysRevLett.48.1425.
- [55] S. Grimme, Semiempirical GGA-type density functional constructed with a long-range dispersion correction, *J. Comput. Chem.* 27 (15) (2006) 1787–1799. doi:10.1002/jcc.20495.
- [56] J. D. Pack, H. J. Monkhorst, Special points for brillouin-zone integrations, *Phys. Rev. B* 16 (1977) 1748–1749. doi:10.1103/PhysRevB.16.1748.
- [57] R. de L. Kronig, On the theory of dispersion of x-rays, *J. Opt. Soc. Am.* 12 (6) (1926) 547–557. doi:10.1364/JOSA.12.000547.
- [58] O. Khyzhun, V. Bekenev, N. Denysyuk, I. Kityk, P. Rakus, A. Fedorchuk, S. Danylchuk, O. Parasyuk, Single crystal growth and the electronic structure of tlpb2br5, *Opt. Mater.* 36 (2) (2013) 251 – 258. doi:<https://doi.org/10.1016/j.optmat.2013.09.004>.
- [59] O. Khyzhun, V. Bekenev, N. Denysyuk, O. Parasyuk, A. Fedorchuk, First-principles band-structure calculations and x-ray photoelectron spectroscopy studies of the electronic structure of tlpb2cl5, *J. Alloys Compd.* 582 (2014) 802 – 809. doi:<https://doi.org/10.1016/j.jallcom.2013.08.127>.
- [60] O. Khyzhun, V. Bekenev, O. Parasyuk, S. Danylchuk, N. Denysyuk, A. Fedorchuk, N. AlZayed, I. Kityk, Single crystal growth and the electronic structure of orthorhombic tl3pbbr5: A novel material for non-linear optics, *Opt. Mater.* 35 (5) (2013) 1081 – 1089. doi:<https://doi.org/10.1016/j.optmat.2012.12.008>.

Improving electron and hole mobility

